Materials Science & Engineering C 118 (2021) 111355

Contents lists available at ScienceDirect

Materials Science & Engineering C

journal homepage: www.elsevier.com/locate/msec

On-stage bioreactor platform integrated with nano-patterned and gold-coated PDMS diaphragm for live cell stimulation and imaging

Yun-Jin Jeong[a,1], Dong-Su Kim[a,1], Jong Yun Kim[a], Nomin-Erdene Oyunbaatar[a], Arunkumar Shanmugasundaram[a], Eung-Sam Kim[b,c], Dong-Weon Lee[a,c,*]

[a] MEMS and Nanotechnology Laboratory, School of Mechanical Engineering, Chonnam National University, Gwangju 61186, Republic of Korea
[b] Department of Biological Sciences, Chonnam National University, Gwangju 61186, Republic of Korea
[c] Center for Next-Generation Sensor Research and Development, Chonnam National University, Gwangju 61186, Republic of Korea

ARTICLE INFO

Keywords:
Stage-top bioreactor
Mechanical stimulation
PDMS diaphragm
Nano-pattern
Maturation
Cardiac cells

ABSTRACT

Over the years, several in-vitro biosensing platforms have been developed for enhancing the maturation of the cultured cells. However, most of the proposed platforms met with limited success due to its inability for live-cell imaging, complicated fabrication, and not being advantageous from an economic perspective due to a higher price. To overcome the drawbacks of the current state-of-the-art, herein, we developed a next-generation stage-top incubator (STI) incorporated with nano grooves patterned PDMS diaphragm (NGPPD). The proposed device consists of a miniatured STI, the NGPPD functional well plates, and a mechanical stimulator. A thin layer of gold (Au) is deposited on the NGPPD to enhanced myogenic differentiation, cell maturation, and cell-cell interactions. The nano grooves are integrated on the PDMS surface to align the cardiomyocytes in the grooved direction during the culture period. The cardiomyocytes cultivated on the Au-deposited NGPPD are stimulated topographically and mechanically during the cultivation period. The enhanced cardiomyocytes maturation cultured on the Au-deposited NGPPD is experimentally demonstrated using immunofluorescence staining and PCR analysis.

1. Introduction

Cells undergo various stimulation to produce multiples of intracellular biological cues in a human body [1,2]. The in-vitro maturation of the cells is prime importance as it has been widely used in various biological applications such as drug toxicity and disease modeling. The mature cells are most desirable to improve the precision of the experimental results of those applications. Therefore, developing a highly effective and efficient bioreactor for in-vitro maturation of heart tissue is imperative for cardiac drug screening applications. To date, several in vitro electrical, mechanical, and electromechanical techniques have been proposed [3–8] to enhance the maturation and contraction force of the cultured cardiomyocytes [9–11].

For instance, Kamotani et al. developed microwell arrays consisting of 24 miniature cell stretching chambers with flexible bottom membranes [12]. The mechanical stimulation was applied for 12 h to the cultured cells using piezoelectrically actuated pins to enhance the cell maturation. The proposed method is not suitable for long-term investigation owing to the friction between the pin and the PDMS membrane. Deguchi et al. developed a piezoelectric actuator-based cell micro stretch device with real-time imaging capability [13]. However, the proposed method is challenging to imply a wide area due to its relatively small driving range. Besides, the developed technique is not advantageous from an economic perspective due to a higher price.

An electromagnetic actuator was proposed for cell maturation by cyclic stretching the flexible cell culture substrate. For example, Chang et al. developed a micropatterned stretching platform to investigate the effect of mechanical stimulation on neural stem cell behavior [14]. Shao et al. developed a uniaxial cell stretching device for live-cell imaging and studied the mechanosensitive cellular functions of the cultured cells [15]. The mechanical stimulations based on electromagnetic motor provided strains in broad ranges and resulted in more accurate experimental results. However, the lubricant used in the electromagnetic motor could result in contamination owing to the highly sensitive cultured cells.

The pneumatic actuators based mechanical stimulation was used for the cell maturation. The pneumatic actuators deformed the cell culture substrate by applying the pressure to the lower part of the membrane.

* Corresponding author at: Center for Next-Generation Sensor Research and Development, Chonnam National University, Gwangju 61186, Republic of Korea.
E-mail address: mems@jnu.ac.kr (D.-W. Lee).
[1] Authors are equally contributed.

https://doi.org/10.1016/j.msec.2020.111355
Received 17 February 2020; Received in revised form 3 July 2020; Accepted 5 August 2020
Available online 11 August 2020
0928-4931/

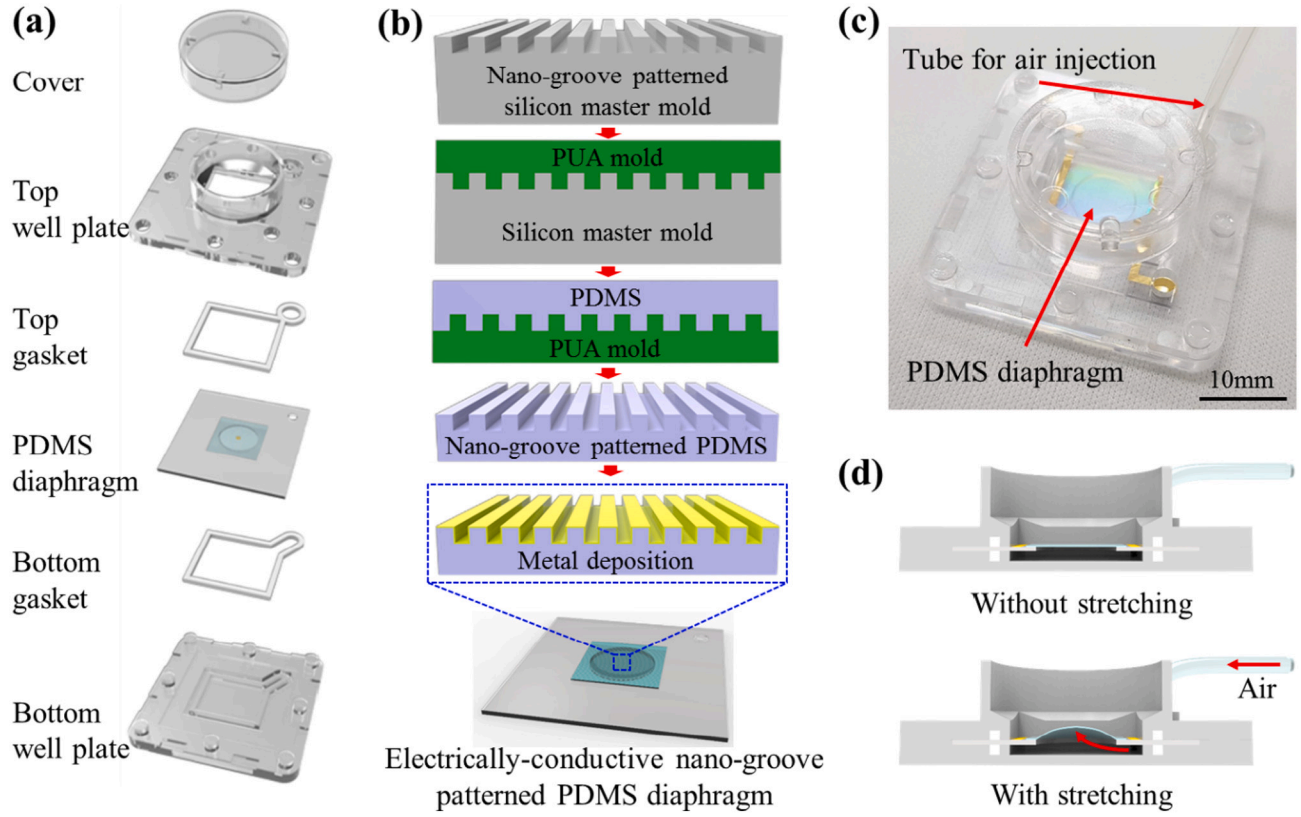

Fig. 1. Schematic illustrating the fabrication process flow and operational principle of the MEMS-based functional well plate. (a) Various parts and assembly processes of a functional well plate, (b) step-by-step fabrication of an Au deposited NGPPD, (c) operational principle and mechanical stimulation of the proposed functional well plate, and (d) photograph of the fabricated functional well plate.

For example, Moraes et al. developed a microfabricated array-based high-throughput screening platform for investigating the cellular response under cyclic mechanical deformation [16]. The lubricant used to minimize the friction between the loading post and the cell culture membrane. However, there is a possibility for cell contamination due to the reaction between the cell culture membrane and silicon-based lubricants [17]. Shimizu et al. proposed a biochip with serially connected pneumatic balloons [18], and various strains were applied in each diaphragm through the pressure drop effect. However, the proposed method is not substantial enough to analyze the conductivity of the cell culture substrate and geometry, and mechanical stimulation of the cultured cardiomyocytes.

Recently, the positively charged polymeric materials such as poly-D-lysine, polylysine, poly-L-ornithine, polyethylenimine, etc. have been used to improve the cell attachment [19–21]. The positively charged polymeric materials enhance the cell adhesion on the culture substrates. However, the polymeric substrates show some undesirable effects on the cultured cells depending on the concentration, exposure time, and charge density [22]. The metal deposited substrates have been used to enhance the cultured cell's myogenic differentiation and maturation. For instance, Yang et al. developed electrically conductive nano-patterned substrates for improved cell maturation. The authors fabricated the nanopatterned PUA using the capillary force lithography technique and subsequently coated with a thin layer of gold or titanium by an electron beam evaporator [23]. Kim et al. used the uniaxially crumpled graphene to enhance cell differentiation and maturation [24].

The commercialized NanoSurface Cytostretcher and FlexCell system have been widely used to enhance the cultured cell maturation. The NanoSurface Cytostretcher consists of the nanopattern functional well plate. The mechanical stimulation was applied to the cells by applying uniaxial stretching. However, the NanoSurfcae cytostretcher does not provide any conductive surface to enhance myogenic differentiation and maturation. In the flexCell system, the mechanical stimulation was applied in biaxial directions using negative air pressure. However, the flexCell system cell culture membrane does not provide any surface topography and electrically conductive substrate for enhancing the cell maturation.

To overcome the drawbacks of the current state-of-the-art, herein, we developed a next-generation stage-top incubator incorporated with nano grooves patterned PDMS diaphragm. The modified photolithography technique was used to fabricate the ~120 μm PDMS diaphragm. The nano grooves were patterned on the PDMS diaphragm for the topographical stimulation of the cultured cardiomyocytes. A thin Au layer was deposited on the NGPPD to enhance cell maturation. The PDMS diaphragm was subjected to mechanical stimulation using a pneumatic pressure pump. The cardiomyocytes obtained from the neonatal rat ventricular myocytes (*NRVM*) isolation were cultured on the developed STI incorporated NGPPD. The simultaneous mechanical and topographical stimulations matured the cultured cells during the cultivation period. The maturation of the cultured cardiomyocytes was systematically analyzed using immunofluorescence staining techniques. The cardiomyocytes cultured on the developed STI incorporated NGPPD under mechanical and topographical stimulations showed much-improved sarcomere length and expression of connexin 43 compared to the control state. Besides, the proposed STI incorporated NGPPD device is capable of real-time live-cell imaging using an optical microscope during the cultivation period. From the obtained results and the potential of the developed bio-sensing platform, we sincerely believe that the designed device could be used in biological as well as regenerative medicine to improve the accuracy of the experimental results.

2. Materials and methods

2.1. Fabrication of MEMS-based functional well plate

Fig. 1 shows a schematic illustration of the proposed STI assembly processes and operation principle of the Au deposited NGPPD. Fig. 1a shows the various parts of the functional well plate. The cover, top, and bottom well plate were prepared by General Purpose Polystyrene (GPPS) material using an injection molding technique (Fig. S1). The silicone rubber gasket was used to fix the PDMS diaphragm rigidly in between the top and bottom well plates. A PDMS was selected as a cell culture substrate owing to the high optical transparency and biocompatibility. The PDMS was spin-coated on the nano-groove patterned PUA mold at 600 rpm and subsequently baking at 80 °C for 1 h using a hotplate. Then, a 120 μm thick nano groove patterned PDMS film was released from the PUA substrate. To further enhance myogenic differentiation, maturation, and intercellular connection, a conductive Ti/Au layer with a thickness of 5 nm and 20 nm was deposited on the nano grooved PDMS using an E-beam evaporator (Fig. 1b). Before the Ti/Au layer deposition, a supportive substrate was attached to the 120 μm thick nano grooved PDMS using the following process. Firstly, a 5 μm thick PDMS layer was spin-coated on the 500 μm silicon wafer followed by baking at 80C for 1 h. Then, a 25 μm thick PI layer was attached to the top surface of the PDMS layer. Subsequently, a 120 μm fabricated nano grooved PDMS was attached on top of the PI layer (Fig. S2).

Recently, several reports have been demonstrated that the O_2 plasma treatment before the metal deposition increases surface roughness, thereby improve the metal layer adhesion on the PDMS substrate [25,26]. In this study, the stable and more adhesive Ti/Au layer on the PDMS substrate was achieved by the optimized O_2 plasma treatment and controlled deposition parameters. Firstly, the nano grooved PDMS substrate was subjected to the O_2 plasma treatment at 200 W for 15 s to increase the surface roughness. Then, a 5 nm thick Ti layer was deposited at the rate of 0.5 Å/s, followed by the deposition of 20 nm thick Au layer at the deposition rate of 1 Å/s. The pressure inside the E-beam evaporator was maintained less than 2×10^{-6} Torr during the deposition process. After the metal deposition, the nanopatterned PDMS film was cut into 1 × 1 cm using a surgical knife. Then the metal-deposited surface was placed top side down position in a through-hole of the JIG, which was manufactured using 3D printing technology. The JIG was used to prevent the PDMS surface from damage where the cells were cultured (Fig. S3).

A plasma bonding (100 W, 60 s) process was carried out to attach the Au deposited PDMS film and a glass plate. The O_2 plasma treatment significantly improved the adhesion between the glass plate and Au deposited PDMS film. The JIG was removed from the top surface to realize the Au deposited NGPPD. The assembled functional well plate outer dimension was ~35 mm in length (l), 35 mm in width (w), and 12 mm in thickness (d), respectively. The diameter of a functional well plate was ~15 mm, and the cardiomyocytes culture area ~ 1.4 cm^2 (Fig. 1c). Fig. 1d shows the mechanical stimulation operation principle of the proposed functional well plate. The Au deposited NGPPD easily deforms according to the applied pressure, which produces a mechanical stimulus to the cultured cardiomyocytes.

2.2. Stage-top incubator system

Fig. S4 in the supporting information shows the schematic illustration of the proposed STI. Fig. S4a shows the STI system's various parts, such as cover, a body, well plate adapter, cover case, printed circuit board (PCB) board, and fluorine-doped tin oxide (FTO) cover glass. The fabricated NGPPD was placed inside the well plate adapter for cell culture and mechanical stimulation. Inside the fabricated STI, three functional well plates were mounted, and the mechanical stimulus was applied simultaneously. The proposed technique provides an opportunity for high throughput cell culture experiments and data acquisition by increasing the STI chamber size and the number of well plate arrays inside the STI. The chamber was covered by an FTO glass cover to observe the cell growth through an optical microscope. The water condensation on the FTO glass cover was prevented by heating the FTO glass cover. A thermistor was used to control the FTO surface temperature. The STI body also consists of a hot water inlet and outlet flow path of diameter 4.2 mm to maintain the inside temperature. The CO_2 concentration inside the bioreactor was kept constant by injecting water vapor consisting of 5% CO_2 through a humidifier. Fig. S4b shows a photograph of the proposed STI. The humidifier and water tank were connected to maintain the constant humidity and temperature inside STI. The water tanks were heated by a cartridge heater (AC 220 V 100 W) and the temperature-controlled by an RTD PT100 temperature sensor. A carbon-filled Teflon was used as a water tank top shield to avoid any temperature-induced distortion. A transparent polycarbonate was used to construct a tank body to verify the amount of water inside the system. The reducer, along with the humidifier, prevents the flow of water droplets into the stage-top incubator through the condensation process. The real-time temperature of the water tank and humidifier was monitored and controlled by the feedback-controlled temperature sensor.

2.3. DC motor-based mechanical stimulator

The air-pump type mechanical stimulator was used to stimulate the cardiomyocytes cultured on the Au-deposited NGPPD. Fig. 2 shows the schematic and photograph of the designed mechanical stimulator contained a small diaphragm-type air pump (DAP-370P, Motro Bank), pressure sensor (33A-005G-2210, Shiba Korea), electronic valve (YYV1-6B, Yingyi motor), AC/DC converter (SFD10-1515, Power Plaza) and motor driver (BA6208, Unisonic Techologeis). The cardiomyocytes cultured undergoes various mechanical stimulation by applying cyclic stretch through the pressure-controlled air pump. The cell culture substrate displacement is controlled by the air pump applied voltage. Further, the NGPPD rise time during the mechanical deformation was controlled by the electronic valve's duty cycle. The tube's size, which was used for the air passage between the mechanical stimulator and the functional well plate, could control the applied pressure and volume. A homemade control program was used to manage the pressure applied by the mechanical stimulator. The real-time force applied by the mechanical stimulator was monitored during the cell culture period. Fig. 2b shows the photograph of the circuit and manufactured controller. The displacement of the Au-deposited NGPPD was measured precisely using a laser vibrometer. The experimental results could be applied to the analytical results to predict the relationship between applied pressure and strain on the diaphragm. Fig. S5 in the supplementary information shows an optical image of a graphical user interface (GUI) made in the laboratory for the mechanical stimulation.

3. Results and discussion

3.1. Stage-top bioreactor integrated with MEMS-based functional well plate arrays

Fig. 3 shows the schematic illustration of a proposed STI incorporated with Au-deposited NGPPD. The device consists of an optical microscope, a functional well plate, an incubator, and an Au-deposited NGPPD. The CO_2 concentration and humidity inside the proposed bioreactor were maintained persistently by continuous passing of 5% CO_2 via a humidifier. The electromagnetic valve was used to control the flow rate of CO_2. The temperature inside a stage-top incubator was controlled by circulating hot water through a mechanical pump. Using the hot water in its place of a conventional electric heater is to minimize the effect of electromagnetic waves on the cultured tissues [27]. The STI was made by an aluminum alloy to absorb heat from the circulating hot water effectively. Also, NGPPD and Au-deposited NGPPD were

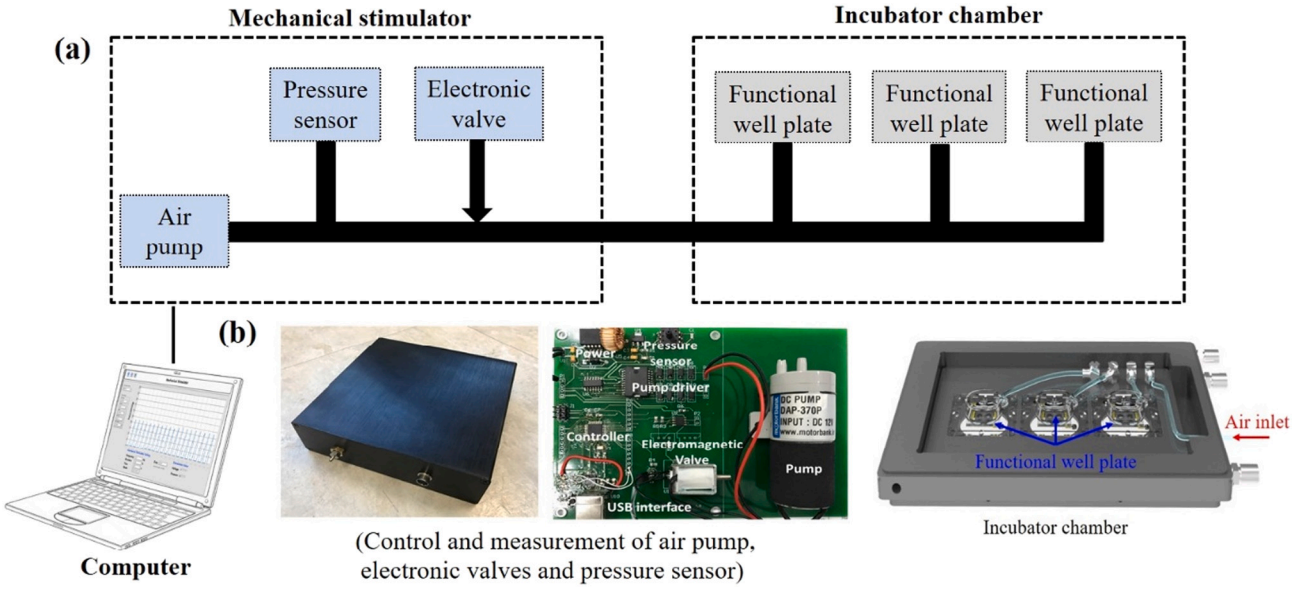

Fig. 2. Schematic and photograph of an electric motor-based air pump system for mechanical stimulation.

positioned center at the proposed bioreactor. The Au and nano grooved patterns were providing the mechanical and topographical stimulations to the cardiomyocytes cultured inside the STI.

Strain analysis of nano-grooves and Au-thin layer deposited PDMS diaphragm.

The strain produced by the NGPPD was investigated using the finite element procedure. The analysis was conducted by fixing one side and applying 2.2 kPa pressure from the center to side edges of the NGPPD (Poisson's ratio: 0.48; Young's modulus: 752 kPa). Fig. 4 depicts the strain and displacement profile of the at 2.2 kPa. The obtained results demonstrate that the radial strain's value was constant with increasing the distance from the center. The negative radial strain was observed at a fixed edge of the NGPPD. The circumferential strain value decreased at a higher distance from the center and attained zero at the fixed side of the NGPPD. The displacement of the NGPPD under 2.2 kPa was measured at different positions from the center. The displacement was decreased from center to edge and showed no displacement at the fixed boundary of the NGPPD. Fig. 4b shows the radial strain ratio to the circumferential strain at 2.2 kPa as a function of NGPPD distance from the center. The radial strain to circumferential strain ratio rose gradually and reached the highest value at 3.5 mm from the center of the NGPPD. The radial strain's value to circumferential strain ratio was from the center to 2.5 mm in the range of 1 to 1.5. Therefore, the cardiomyocytes cultured in the NGPPD surrounded by a radius of 2.5 mm from the center was considered for further analysis.

3.2. Characterization of stage-top incubator and mechanical stimulator

The temperature and humidity measurement system was constructed to analyze the temperature and humidity characteristics according to the internal position of the STI. The measurement system was manufactured to be the same size as the commercial well plate and could be mounted inside the incubator. Fig. S6a shows the schematic of the placement of temperature and humidity sensors. The numerical 1 to 5 were indicating the placement of temperature and humidity sensor inside the STI. The sensors were fixed in different places to measure the

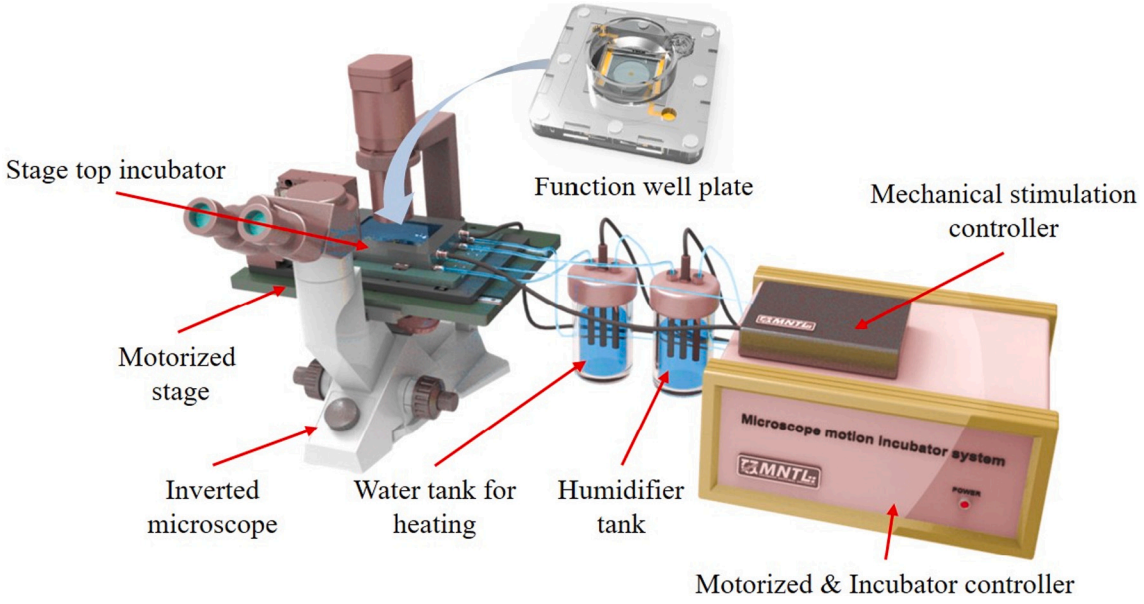

Fig. 3. Schematic illustration of a proposed STI combined with Au-deposited NGPPD for geometrical, and mechanical stimulation.

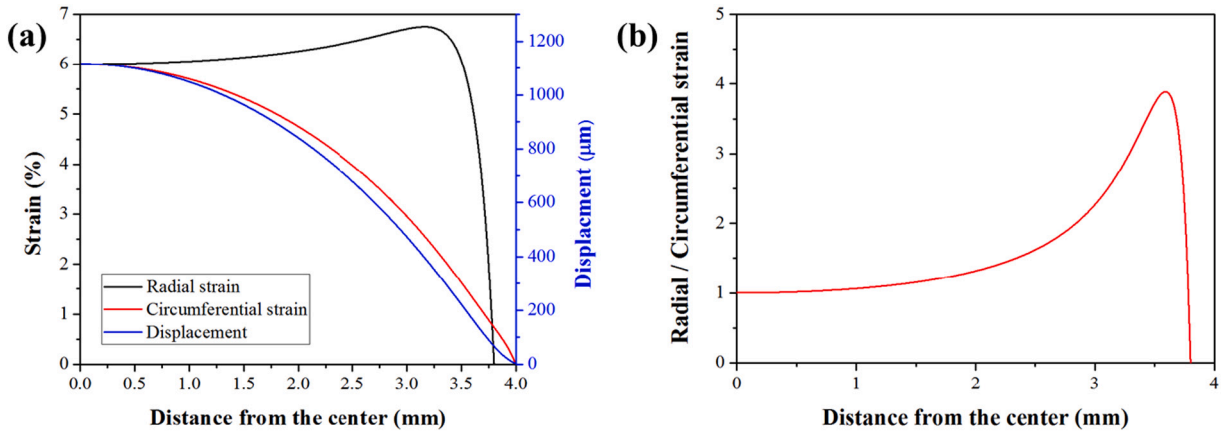

Fig. 4. Simulation data obtained from finite elemental analysis. (a) Strain and displacement profiles of the NGPPD at 2.2 kPa, (b) ratio of the circumferential strain to the radial strain under 2.2 kPa.

temperature and the humidity gradient in the STI interior. The temperature inside the bioreactor was maintained at 37 °C as the cells were cultured at that temperature.

Fig. S6(b, c) shows the measured temperature and humidity inside the STI at different times. The temperature inside the STI increases with increasing time and attain the set value approximately in 60 min and then maintained constant. The inset in Fig. S6b shows the inside STI temperature at different places. The average temperature distribution inside the STI was ~36.92 ± 0.26 °C. The small variation in the temperature could be attributed to the hot water circulation. The temperature measured at the inlet side of the hot water was high, and the temperature measured at the outlet side was low. The small variation in the temperature difference was negligible and could be ignored during cell culture. Fig. S6c shows the humidity inside the STI as a function of time. The humidity inside the STI increased with time and saturated in 50 min and kept constant with further increasing time. The CO_2 concentration inside the STI was maintained constant by continuously injecting 5% gas through the humidifier.

The Au-deposited NGPPD vertical displacement was measured using a laser displacement sensor (LK-G30, Keyence, Osaka, Japan). A laser vibrometer measured the Au-deposited NGPPD displacement at a different duty cycle, applied voltage, and tube volume of the mechanical stimulator. Fig. 5a shows the normalized displacement of the NGPPD at different duty cycles ranging from 1 to 50% of the electrical power applied to the motor. The rising and decay time of the Au-deposited NGPPD during the mechanical deformation increased according to the duty cycle at 1 Hz of the mechanical stimulator. The shape of the stimulus was similar to that of the commercial stimulator using a conventional linear motor at 50% of the duty cycle. Therefore, additional experiments were conducted with a duty cycle of 50% by varying the applied voltage.

Fig. S7 in the supplementary information shows the displacement of the Au-deposited NGPPD as a function of applied DC bias and duty cycle. The displacement was increased by increasing the DC bias and duty cycle. Fig. 5b shows the displacement with different tube volumes (10 mL and 50 mL) at a different applied voltage. The displacement was increased by increasing the applied voltage. Fig. S8 shows corresponding strain value, which was estimated using a finite element method. The displacement and strain of the Au-deposited NGPPD at 3–5 V were in the range of ~1460–2112 μm and ~11–23%, respectively, at 10 mL of the tube volume. Whereas, the displacements and strain of the PDMS diaphragm were ~1060–1400 μm and ~5.4–9.4% at 50 mL of the tube volume. The preliminary experiments were verified that the different strains could be produced by varying the tube volume and voltage applied to the air pump. Fig. S9a in the supplementary information shows the photograph of the Au-deposited NGPPD with and without stretch. Fig. S9b shows the displacement of the Au-deposited NGPPD at 1 Hz frequency and a 6% strain (Movie S1).

3.3. Cell immunofluorescence staining

Well-organized sarcomeres are an essential factor for cardiac cell maturation and maximizing cardiomyocyte contractility [28]. The cardiomyocytes obtained from NRVM isolation is briefly described in the supplementary information [29]. The acquired cardiomyocytes were cultured on the grooved PDMS membrane with different dimensions such as 800 nm, 1.2 μm, and 1.5 μm. Fig. S10 shows the SEM image of the 800 nm grooved PDMS membrane at different magnifications. Fig. S11 shows the optical images of the cardiomyocytes cultured on the flat and nano grooved PDMS membrane. The optical images showed the alignment of the cardiomyocytes in the groove directions. The cardiomyocytes were also cultured on the flat PDMS membrane to compare for the controlled experiment. The cardiomyocytes were cultured on the PDMS membrane with and without nano grooves for 10 days.

The alignment of the cultured cardiomyocytes was verified by periodic evaluations using a confocal microscope. An immunofluorescence staining analysis was performed to analyze the sarcomere length of the cultured cardiomyocytes on day 7. Fig. S12 shows the staining images and sarcomere length of the cardiomyocytes cultured on the different grooved PDMS membrane. The cardiomyocytes cultured on the 800 nm grooved PDMS membrane exhibited more alignment than the 1.2 μm and 1.5 μm grooved PDMS membrane. The sarcomere length of the cardiomyocytes cultured on the 800 nm, 1.2 μm, and 1.5 μm grooved PDMS membrane was ~1.85 ± 0.04 μm, 1.81 ± 0.03 μm and 1.78 ± 0.03 μm, respectively. Among different grooved PDMS membrane, an 800 nm groove was most efficient for the cell maturation. The obtained data were consistent with the previous reports [30].

The alignment of the cultured cardiomyocytes was verified by periodic evaluations using a confocal microscope. An immunofluorescence staining analysis was performed to analyze the sarcomere length of the cultured cardiomyocytes on day 10. Fig. 6 shows the immunofluorescence images and sarcomere length of the cardiomyocytes cultured on the PDMS membrane with and without nano grooves. Fig. 6a shows the α-actinin of the cardiomyocytes cultured on the flat and grooved PDMS membrane. The aligned α-actinin was observed for the cardiomyocytes cultured on the 800 nm grooved PDMS membrane. Whereas, the cardiomyocytes on the flat PDMS membrane was grown randomly. The sarcomere length of the cardiomyocytes cultured on the flat and nano grooved PDMS was ~1.69 ± 0.05 μm and 1.85 ± 0.04 μm, respectively. The higher the sarcomere length is indicating, the more maturation of the cultured cardiomyocytes.

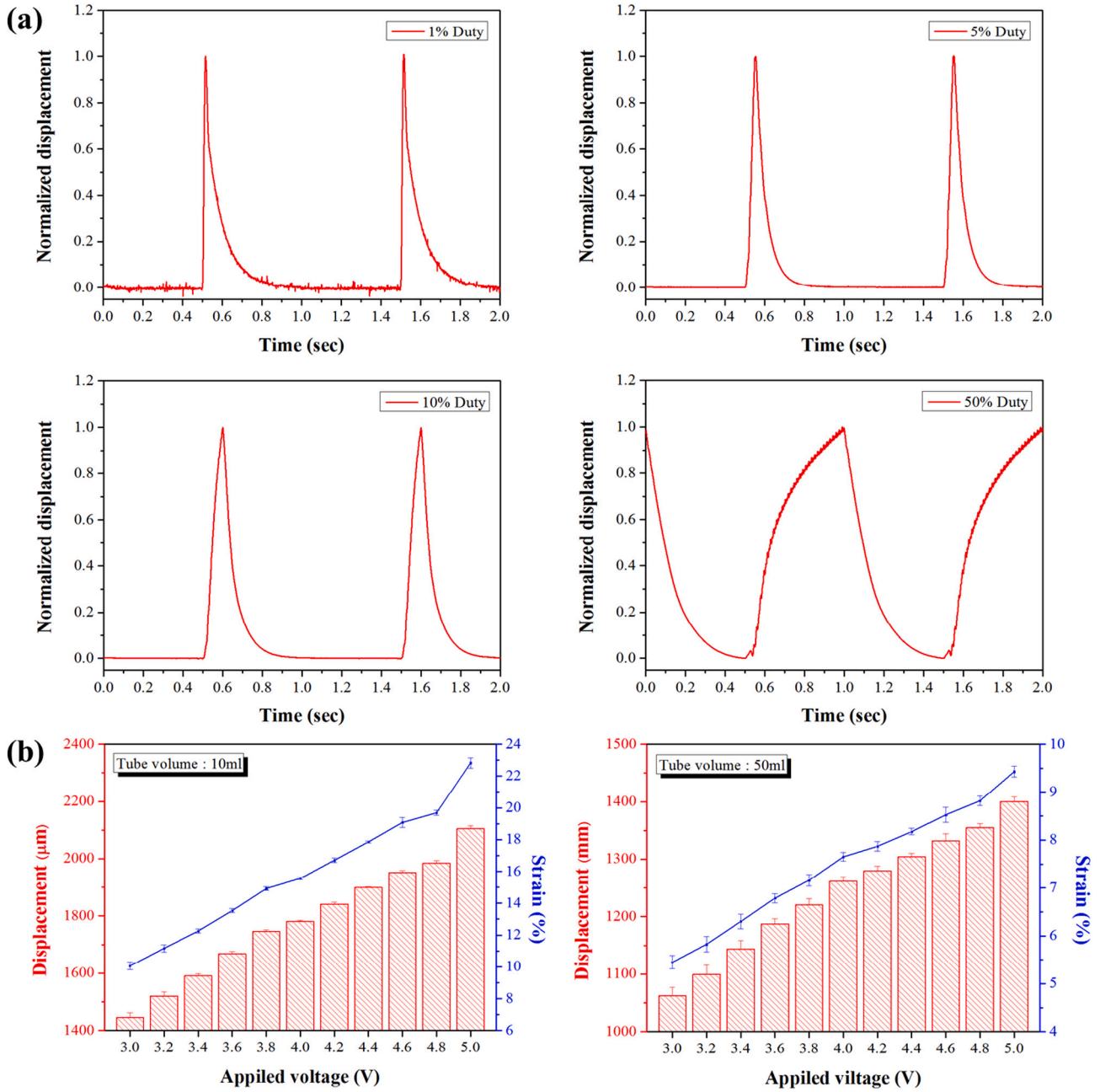

Fig. 5. (a) Displacement of the Au-deposited NGPPD at different duty cycles (1 to 50%) of the mechanical stimulator. (b) Au-deposited NGPPD displacement and corresponding strain at different applied voltages with varying tube volumes (10 and 50 mL). Error bars are mean ± s.d. (n = 5).

The wettability of the substrate significantly influences the cell adhesion on the cell culture substrate [31]. In general, O_2 treatment is performed to modify the surface properties of substrates before the ECM coating. However, most of the cell culture substrates are recovered to their original features within 3 days. The inherent hydrophobic nature of the PDMS tends to exacerbate the adhesion of the cardiac cells. Regularly repeated shrinkage and relaxation in cardiac cells make this problem even more severe. Fig. 7a shows the water contact angles (WCA) of the flat and nano-grooved PDMS substrates with and without Au coating. The WCA of the flat and nano-grooved PDMS was ~112.5 ± 0.85° and 128.5 ± 4.4°, respectively. Whereas, the WCA of the flat and nano-grooves patterned PDMS with and without Au deposition was 47.4 ± 4.1° and 73.4 ± 1.1°, respectively. Cell adhesion was reported to be best when the culture substrate's water contact angle was between 60° and 80° [32]. Therefore, cardiac cell adhesion was expected to be improved on the Au-deposited PDMS nano-groove surface.

Fig. 7b shows the cell densities of the cultured cardiomyocytes on the bare flat and nano grooved PDMS membrane, and Au deposited fat and nano grooved PDMS membrane. The cell density was defined as the number of nuclei within the unit area (mm^2). The cell densities on the flat and nano grooved PDMS were ~1237.2 ± 211.4 and 1316.4 ± 198.5, respectively. Whereas, the cell densities on the Au deposited flat and nano grooved PDMS were ~1691.8 ± 129.6 and 1671.2 ± 182.2, respectively. There were no significant differences in cell densities observed between the flat and nano grooved PDMS and Au deposited flat and nano grooved PDMS. However, significant differences were observed in the cardiomyocyte's densities cultured on the bare and Au deposited PDMS membrane, and the DAPI staining analysis further confirms it. Fig. S13 shows the DAPI staining images of the cardiomyocytes cultured on the bare and Au deposited PDMS membrane. The number of nuclei in each group was measured in an area of

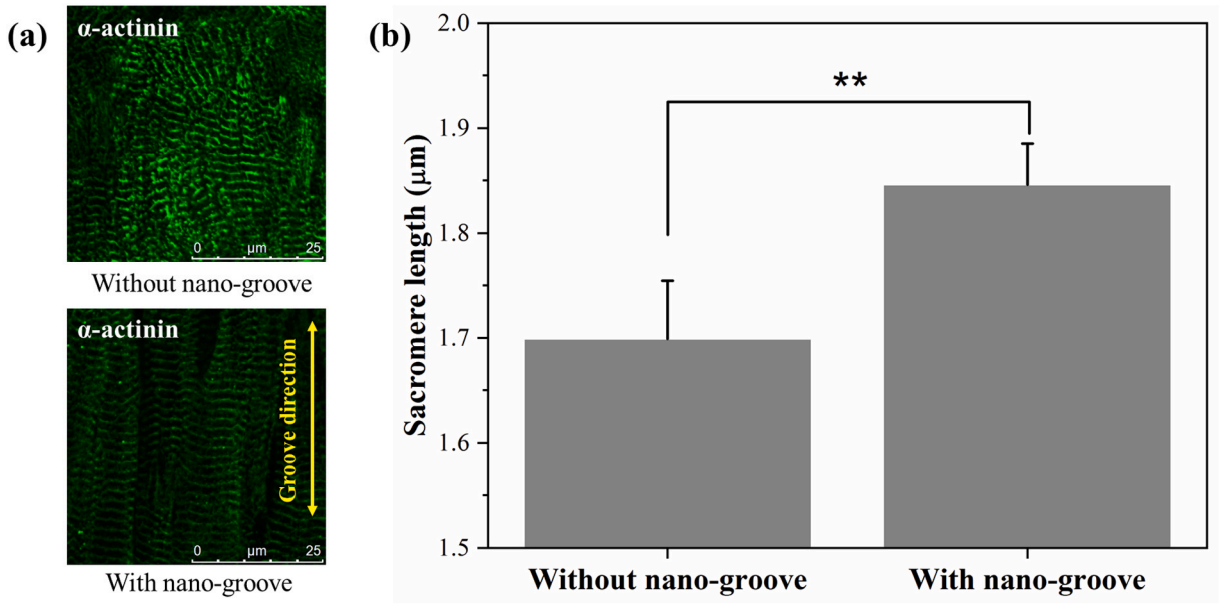

Fig. 6. (a) Immunofluorescence staining images of the cardiomyocytes cultured on the PDMS diaphragm with and without nanogroove. (b) Sarcomere length of the cardiomyocytes cultured on the PDMS diaphragm with and without nano grooves. Error bars are mean ± s.d., (n = 5). $^{**}P < 0.01$.

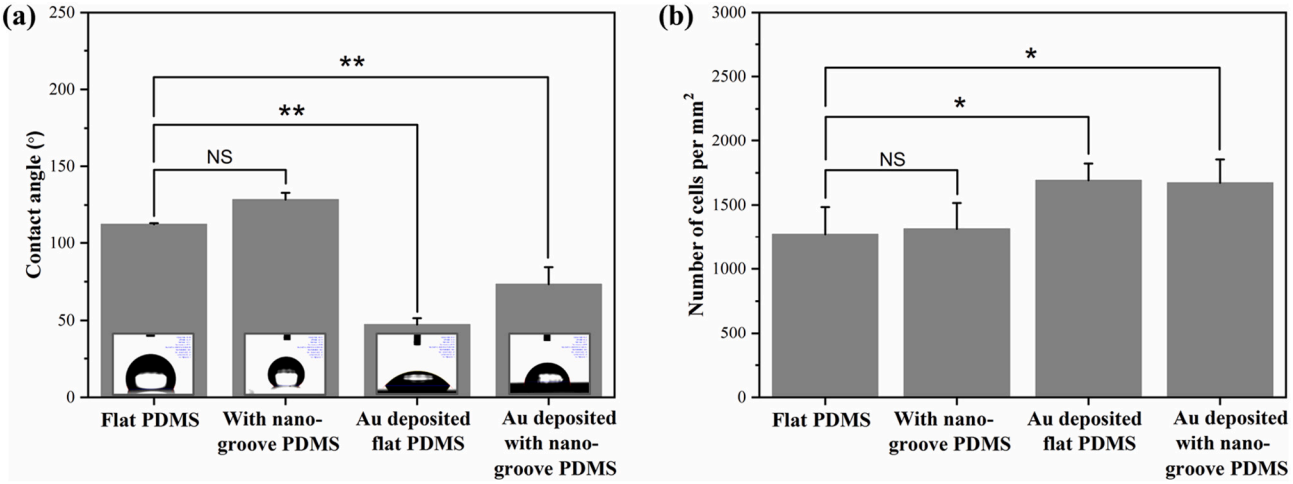

Fig. 7. (a) Water contact angles of the flat and nano-groove patterned PDMS substrate with and without Au coating. Error bars are representing mean ± s.d., n = 3, $^{**}P < 0.01$ measures by one-way ANOVA followed by Tukey's honest significant difference test. (b) Cultured cardiomyocytes densities on the bare flat and nanogrooved PDMS and Au deposited flat and nanogrooved PDMS. Error bars are representing mean ± s.d., n = 5, $^{*}P < 0.05$ measures by one-way ANOVA followed by Tukey's honest significant difference test. NS is non-significant.

250 μm × 250 μm. The amount of DAPI was increased ~21% on the Au-deposited PDMS surface compared to pure PDMS, indicating that the electrically conductive culture substrate influences the cell growth during the culture day. The PCR analysis confirmed the enhanced cardiomyocyte's maturation cultured on the Au-deposited PDMS membrane (Fig. S14). The RT-qPCR of the three genes analysis verifies the improved contraction force (MHC 6, cTnT), superior cell maturation (α-actinin). The MHC6 of cardiomyocytes cultured on bare and Au deposited NGPPD on day 10 were found to be 0.028 ± 0.011 and 0.07 ± 0.002. The α-actinin of the cardiomyocytes cultured was 0.229 ± 0.029 and 1.344 ± 0.059, respectively. The cTnT of the cardiomyocytes cultured on the Au-deposited PDMS membrane significantly improved than bare PDMS membrane.

Additional experimental analysis was performed to evaluate the impact of mechanical stimulation (1 Hz, stretching rate 6%, 50% duty cycle and mechanical stimulator tube volume is 50 mL) on the cultured cardiomyocytes. Fig. S15 shows the photograph of the cardiomyocytes cultured Au-deposited NGPPD with and without mechanical stimulation (Movie S2). The cardiomyocytes were cultured on the Au-deposited NGPPD for 10 days without any mechanical stimulations as a control. Whereas, the cardiomyocytes cultured on the Au-deposited NGPPD was subjected to the mechanical stimulation at 1 Hz from the 4th day of the culture period. Investigation of α-actinin and Cx43 protein expression is essential for analyzing the sarcomeres length and intercellular interaction of the cultured cardiomyocytes. Fig. S16 shows the beat rate of the cardiomyocytes cultured on the Au deposited NGPPD as a function of the culture period. The cardiomyocytes' beating rate was increased until the 6th day of the culture period and then decreased. The beating rate of cardiomyocytes significantly decreased at a higher culture period indicative of more maturation of cardiomyocytes. Fig. S17 shows the cardiomyocytes beat rate on day 10 cultured under 1 Hz mechanical stimulation. The beat rate of the cardiomyocytes without mechanical stimulation was ~0.68 ± 0.12 Hz, whereas, the beat rate of the cardiomyocytes cultured under 1 Hz of mechanical stimulation was

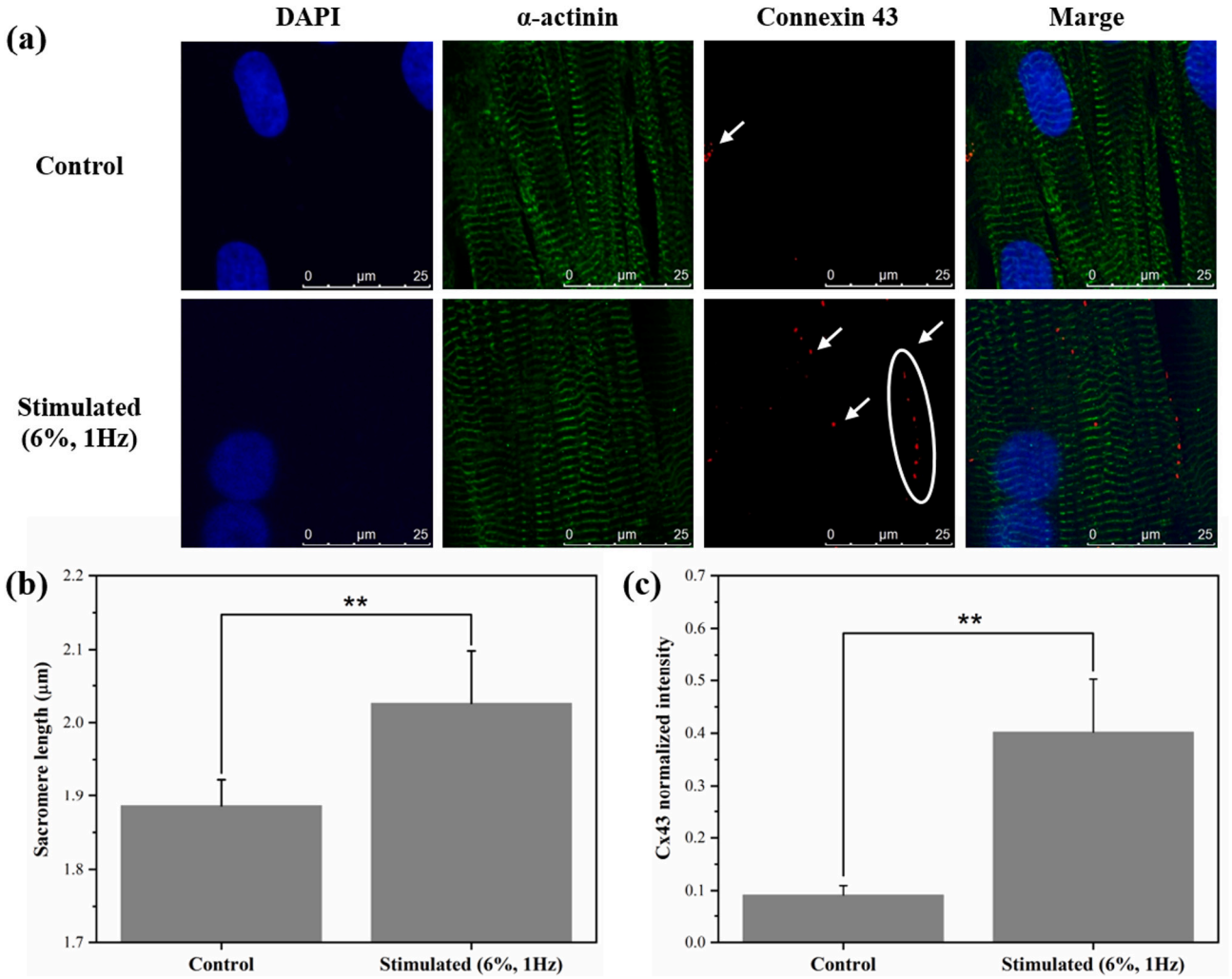

Fig. 8. Immunofluorescence images of the cultured cardiomyocytes with and without mechanical stimulations. (a) ICC protein expression (nucleus-blue, α-actinin-green, and Cx43-red), (b), and (c) Sarcomere length and Cx43 of the cardiomyocytes cultured with and without mechanical stimulations. Error bars are mean ± s.d., (n = 10). $^{**}P < 0.01$. (For interpretation of the references to color in this figure legend, the reader is referred to the web version of this article.)

~0.97 ± 0.08 Hz.

The maturation of the cultured cardiomyocytes was investigated using immunofluorescent staining analysis on day 10 of the cultured period (Fig. 8). The staining images were analyzed by measuring the fluorescence intensity through a software Image J. The staining images demonstrated that the DAPI, α-actinin, and Cx43 of the cardiomyocytes cultured under the mechanical stimulation more enhanced compared to that of the control state. Fig. S18 the cardiomyocytes sarcomeres length and Cx43 under 1 Hz mechanical stimulation at different cultured days. The sarcomere length and Cx43 of the cardiomyocytes on day 4, 7 and 10 were found to be ~1.92 ± 0.063 μm, 2.02 ± 0.072 μm, and 2.04 ± 0.079 μm and 0.211 ± 0.017, 0.401 ± 0.100, and 0.415 ± 0.119, respectively. Fig. 8b shows the cardiomyocytes sarcomeres cultured on the Au-deposited NGPPD with and without mechanical stimulation. The sarcomere length of the cardiomyocytes cultured under the mechanical stimulus is ~10.7% higher than that of the control state (without mechanical stimulations). Fig. 8c shows the Cx43 of the cardiomyocytes cultured under the mechanical stimulus and without mechanical stimulations. The normalized Cx43 intensity of the cultured cardiomyocytes with mechanical stimulations and control state was found to be 0.0913 ± 0.0182 and 0.4032 ± 0.1005, respectively. The experimental analysis has been repeated more than three-times using the biologically independent sample to confirm the reliability of the obtained data.

The enhanced cardiomyocytes maturation cultured on the Au deposited NGPPD on day 10 under 1 Hz mechanical stimulation was investigated using PCR analysis (Fig. S19). The MHC6 of the cardiomyocytes under mechanical stimulation was increased from 0.07 ± 0.002 to 0.309 ± 0.009. The α-actinin of cardiomyocytes with and without mechanical stimulation on day 10 were ~1.344 ± 0.059 and 6.75 ± 0.059, respectively. Whereas the cTnT expression of the cardiomyocytes on day 10 was increased to 4.717 ± 0.438 compared to the control state (2.098 ± 0.195). The PCR analysis demonstrated the enhanced maturation and contractility of the cardiomyocytes cultured under 1 Hz of mechanical stimulation.

4. Conclusions

We developed a next-generation STI incorporated with an Au-deposited NGPPD for culturing the cardiomyocytes. The humidity and temperature inside the STI were maintained constant by a humidifier, and continuous circulation of hot water. The temperature and humidity sensors were fixed at five different positions to precisely measure the temperature and humidity gradients inside the STI. The STI was heated through the hot water circulation to minimize the electromagnetic effect on the cultured cardiomyocytes. The nano grooves were patterned on the PDMS diaphragm for aligning the cells in the grove directions. The Au layer was deposited on the PDMS membrane to enhance the

cultured cell's myogenic differentiation and maturation. The ability of the dual mechanical and topographical stimulations of the developed bioreactor significantly increased the maturation of the cultured cardiomyocytes. Finally, the improved maturation of the cardiomyocytes cultured on the developed STI incorporated with Au-deposited NGPPD was demonstrated by staining and PCR analysis. The proposed device could be applied in several fields of regenerative medicine and other biological applications.

Supplementary data to this article can be found online at https://doi.org/10.1016/j.msec.2020.111355.

CRediT authorship contribution statement

Yun-Jin Jeong:Methodology, Data curation, Writing - original draft.**Dong-Su Kim**:Methodology, Data curation, Writing - original draft.**Jong Yun Kim**:Investigation.**Nomin-Erdene Oyunbaatar**:Investigation.**Arunkumar Shanmugasundaram**:Data curation, Writing - original draft.**Eung-Sam Kim**:Data curation.**Dong-Weon Lee**:Data curation, Writing - original draft.

Declaration of competing interest

The authors declare that they have no known competing financial interests or personal relationships that could have appeared to influence the work reported in this paper.

Acknowledgments

This study was supported through a National Research Foundation of Korea (NRF) grant funded by the Korean government (MSIT) (No. 2017R1E1A1A01074550) and Basic Science Research Program through a National Research Foundation of Korea (NRF) funded by the Ministry of Education (No. 2019R1A6A3A01097112).

References

[1] F.H. Silver, L.M. Siperko, Mechanosensing and mechanochemical transduction: how is mechanical energy sensed and converted into chemical energy in an extracellular matrix? Crit. Rev. Bioeng. 31 (2003) 255–334.
[2] R.P. Brandes, N. Weissmam, K. Schröder, Nox Family NADPH oxidases in Mechanotransduction: mechanisms and consequences, Antioxid. Redox Signal. 20 (2014) 887–898.
[3] N. Tandon, A. Marsano, R. Maidhof, L. Wan, H. Park, G. Vunjak-Novakovic, Optimization of electrical stimulation parameters for cardiac tissue engineering, J. Tissue Eng. Regen. Med. 5 (2011) 115.
[4] A. Sathaye, N. Bursac, S. Sheehy, L. Tung, Electrical pacing counteracts intrinsic shortening of action potential duration of neonatal rat ventricular cells in culture, J. Mol. Cell. Cardiol. 41 (2006) 633.
[5] N. Tandon, C. Cannizzaro, P.-H.G. Chao, R. Maidhof, A. Marsano, H.T.H. Au, M. Radisic, G. Vunjak-Novakovic, Electrical stimulation systems for cardiac tissue engineering, Nat. Protoc. 4 (2009) 155.
[6] S.S. Nunes, J.W. Miklas, J. Liu, R. Aschar-Sobbi, Y. Xiao, B. Zhang, J. Jiang, S. Massé, M. Gagliardi, Biowire: a platform for maturation of human pluripotent stem cell-derived cardiomyocytes, Nat. Methods 10 (2013) 781.
[7] M. Shachar, N. Benishti, S. Cohen, Effects of mechanical stimulation induced by compression and medium perfusion on cardiac tissue engineering, Biotechnol. Prog. 28 (2012) 1551.
[8] P. Akhyari, P.W. Fedak, R.D. Weisel, T.-Y.J. Lee, S. Verma, D.A. Mickle, R.K. Li, Mechanical stretch regimen enhances the formation of bioengineered autologous cardiac muscle grafts, Circulation 106 (2002) 137–142.
[9] N.L. Tulloch, V. Muskheli, M.V. Razumova, F.S. Korte, M. Regnier, K.D. Hauch, L. Pabon, H. Reinecke, C.E. Murry, Growth of engineered human myocardium with mechanical loading and vascular coculture, Circ. Res. 109 (2011) 47–59.
[10] C. Fink, S.L. ERGÜN, D. Kralisch, U. Remmers, J. Weil, T. Eschenhagen, Chronic stretch of engineered heart tissue induces hypertrophy and functional improvement, FASEB J. 14 (2000) 669–679.
[11] T. Zhang, L.Q. Wan, Z. Xiong, A. Marsano, R. Maidhof, M. Park, Y. Yan, G. Vunjak-Novakovic, Channelled scaffolds for engineering myocardium with mechanical stimulation, J. Tissue Eng. Regen. Med. 6 (2012) 748–756.
[12] Y. Kamotani, T. Bersano-Begey, N. Kato, Y.-C. Tung, D. Huh, J.W. Song, S. Takayama, Individually programmable cell stretching microwell arrays actuated by a Braille display, Biomaterials 29 (2008) 2646–2655.
[13] S. Deguchi, S. Kudo, T.S. Matsui, W. Huang, M. Sato, Piezoelectric actuator-based cell microstretch device with real-time imaging capability, AIP Adv. 5 (2015) 067110.
[14] Y.-J. Chang, C.-J. Tsai, F.-G. Tseng, T.-J. Chen, T.-W. Wang, Micropatterned stretching system for the investigation of mechanical tension on neural stem cells behavior, Nanomedicine 9 (2013) 345–355.
[15] Y. Shao, X. Tan, R. Novitski, M. Muqaddam, P. List, L. Williamson, J. Fu, A.P. Liu, Uniaxial cell stretching device for live-cell imaging of mechanosensitive cellular functions, Rev. Sci. Instrum. 84 (2013) 114304.
[16] C. Moraes, J.-H. Chen, Y. Sun, C.A. Simmons, Microfabricated arrays for high-throughput screening of cellular response to cyclic substrate deformation, Lab Chip 10 (2010) 227–234.
[17] Y. Huang, N.-T. Nguyen, A polymeric cell stretching device for real-time imaging with optical microscopy, Biomed. Microdevices 15 (2013) 1043–1054.
[18] K. Shimizu, A. Shunori, K. Morimoto, M. Hashida, S. Konishi, Development of a biochip with serially connected pneumatic balloons for cell-stretching culture, Sensors Actuators B Chem. 156 (2011) 486–493.
[19] H.-J. Cho, H.-J. Lee, Y.-J. Chung, J.-Y. Kim, H.-J. Cho, H.-M. Yang, Y.-W. Kwon, H.-Y. Lee, B.-H. Oh, Y.-B. Park, H.-S. Kim, Generation of human secondary cardiospheres as a potent cell processing strategy for cell-based cardiac repair, Biomaterials 34 (2013) 651–661.
[20] B. Peña, V. Martinelli, M. Jeong, S. Bosi, R. Lapasin, M.R.G. Taylor, C.S. Long, R. Shandas, D. Park, L. Mestroni, Biomimetic polymers for cardiac tissue engineering, Biomacromolecules 17 (2016) 1593–1601.
[21] E. Tomecka, M. Wojasinski, E. Jastrzebska, M. Chudy, T. Ciach, Z. Brzozka, Poly(l-lactic acid) and polyurethane nanofibers fabricated by solution blow spinning as potential substrates for cardiac cell culture, Mater. Sci. Eng. C 75 (2017) 305–316.
[22] D. Fischer, Y. Li, B. Ahlemeyer, J. Krieglstein, T. Kissel, In vitro cytotoxicity testing of polycations: influence of polymer structure on cell viability and hemolysis, Biomaterials 24 (2003) 1121–1131.
[23] H.S. Yang, B. Lee, J.H. Tsui, J. Macadangdang, S.Y. Jang, S.G. Im, D.H. Kim, Electroconductive nanopatterned substrates for enhanced myogenic differentiation and maturation, Adv. Healthcare Mater. 5 (2016) 137–145.
[24] J. Kim, J. Leem, H.N. Kim, P. Kang, J. Choi, M.F. Haque, D. Kang, S. Nam, Uniaxially crumpled graphene as a platform for guided myotube formation, Microsyst. Nanoeng. 5 (2019) 53.
[25] J.Y. Baek, G.H. Kwon, J.Y. Kim, J.H. Cho, S.H. Lee, K. Sun, S.H. Lee, Stable deposition and patterning of metal layers on the PDMS substrate and characterization for the development of the flexible and implantable micro electrode, Solid State Phenom. 124 (2007) 165–168.
[26] O. Graudejus, P. Gorrn, S. Wagner, Controlling the morphology of gold films on poly(dimethylsiloxane), ACS Appl. Mater. Interfaces 2 (2010) 1927–1933.
[27] J. Ameen, Reduction of cell phone electromagnetic radiation effect on human body, Inter. J. Sci. 3 (2014) 19–23.
[28] W.L. Stoppel, D.L. Kaplan, L.D. Black III, Electrical and mechanical stimulation of cardiac cells and tissue constructs, Adv. Drug Deliv. Rev. 96 (2016) 135–155.
[29] D.-S. Kim, Y.-J. Jeong, B.-K. Lee, A. Shanmugasundaram, D.-W. Lee, Piezoresistive sensor-integrated PDMS cantilever: a new class of device for measuring the drug-induced changes in the mechanical activity of cardiomyocytes, Sensors Actuators B Chem. 240 (2017) 566–572.
[30] D. Carson, M. Hnilova, X. Yang, C.L. Nemeth, J.H. Tsui, A.S. Smith, A. Jiao, M. Regnier, C.E. Murry, C. Tamerler, D.H. Kim, Nanotopography-induced structural anisotropy and sarcomere development in human cardiomyocytes derived from induced pluripotent stem cells, ACS Appl. Mater. Interfaces 8 (2016) 21923–21932.
[31] D. Fuard, T. Tzvetkova-Chevolleau, S. Decossas, P. Tracqui, P. Schiavone, Optimization of poly-di-methyl-siloxane (PDMS) substrates for studying cellular adhesion and motility, Microelectron. Eng. 85 (2008) 1289–1293.
[32] Y. Tamada, Y. Ikada, Cell adhesion to plasma-treated polymer surfaces, Polymer 34 (1993) 2208–2212.